CVPR #12127

DL2G: Degradation-guided Local-to-Global Restoration for Eyeglass Reflection Removal

Supplementary Material

In the supplementary material, we first present additional comparison results on eyeglass reflection images collected under the controlled lighting conditions, including the visualization results on the original ReyeR dataset [8] and on our supplementary images. Then, we provide more visualization results on the eyeglass reflection images collected from the Internet, where the lighting conditions are uncontrolled, to show the generalization ability of our method. We also try to use our method to deal with the high-resolution images with eyeglass reflection. Lastly, we provide more results on highlight specular images.

1. Additional Results on Eyeglass Reflection Images under Controlled Lighting Conditions

1.1. Visualization Results of the Degradation Model

In Fig.1, we present four groups of results to show the effects of our proposed degradation model for reflection alleviation. It can be seen that the proposed degradation estimation module (DEM) can predict the degradation map accurately. It is rather effective to use the proposed degradation model to alleviate the degradation, and to guide the following local-to-global restoration.

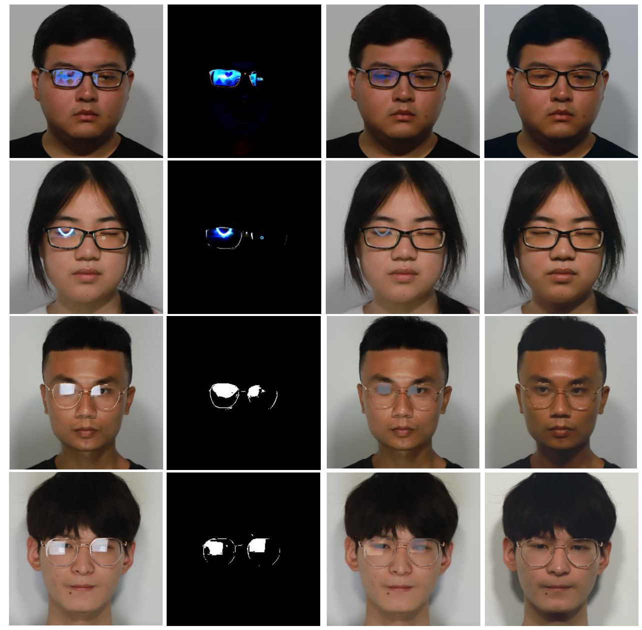

(a) (b) (c) (d)

Figure 1. Visualization results of the degradation model. (a) Input image, (b) predicted degradation map D, (c) the preliminary result $\widetilde{T}$, (d) GT.

1.2. Comparison Results on ReyeR Dataset

We provide more qualitative results on the original ReyeR dataset in Fig. 2, and make comparisons with two eyeglass reflection removal methods Watanabe *et al.* [6] and ER^{2}Net [8], three advanced image reflection removal methods IBCLN [4], DSRNet [3] and Robust SIRR [5].

From Fig.2, we can see that although the comparison methods can remove the weak and small-area reflection (see the results in the third row), they tend to leave some residuals (see the results in the first row) or generate blurry contents in the strong reflective area (see the results in the second row). Our method can remove the reflections and restore the clear and accurate details in the strong reflective area.

1.3. More Visualization Results on ReyeR+ Dataset

We also present more visualization results on our supplementary images to show the performance of our method on more challenging reflection situations. From Fig. 3, we can see the comparison methods cannot remove the reflections completely (see the results in the first and the third rows), and the generated results often contain visual artifacts (see the results in the last two rows). Our method can remove the reflections completely and generate semantic reasonable results without visual artifacts.

2. More Visualization Results on images collected from the Internet

We evaluate the generalization ability of our method on the images collected from the Internet, and present the comparison results in Fig.4 and Fig.5. It can be seen that the comparison methods struggle to remove reflections completely, restore the lost contents reasonably, and generate detailed images without artifacts. Our method is more robust to reflection intensity and color, degradation area and complex backgrounds. All the results demonstrate that our method can be generalized to indoor and outdoor scenes with complex reflections.

3. Performance on High-Resolution Images

In practical applications, there is a significant demand for high-resolution image processing. However, when apply-

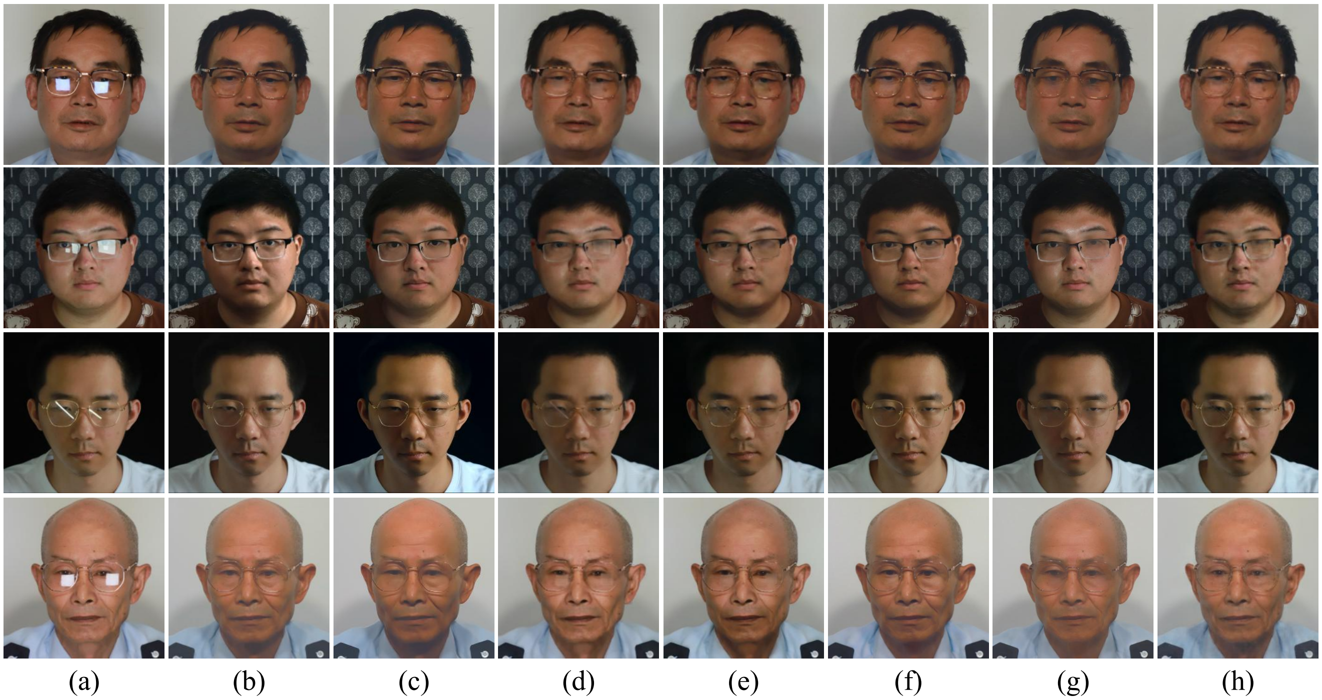

Figure 2. Qualitative comparison with other methods on images collected from the Internet. (a) Input image, (b) Ours, (c) Watanabe *et al.* [6], (d) IBCLN [4], (e) Robust SIRR [5], (f) DSRNet [3], (g) ER^2Net [8].

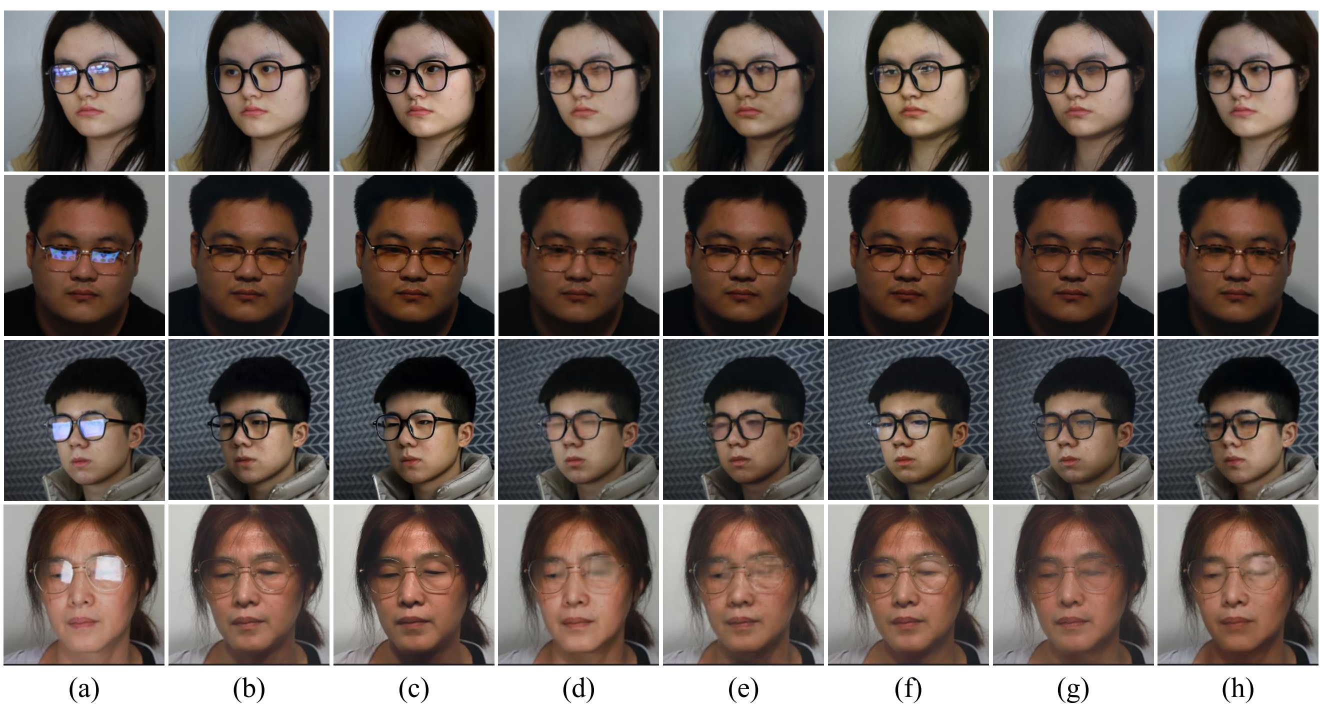

Figure 3. Visualization results on images in the ReyeR+ dataset. (a) Input image, (b) Ours, (c) Watanabe *et al.* [6], (d) IBCLN [4], (e) Robust SIRR [5], (f) DSRNet [3], (g) ER^2Net [8].

ing existing methods to process of high-resolution images, there is a limit to the resolution that can be handled. We have tested that, on an NVIDIA GeForce RTX 3090 graphics card, DSRNet [3] can only process images up to a

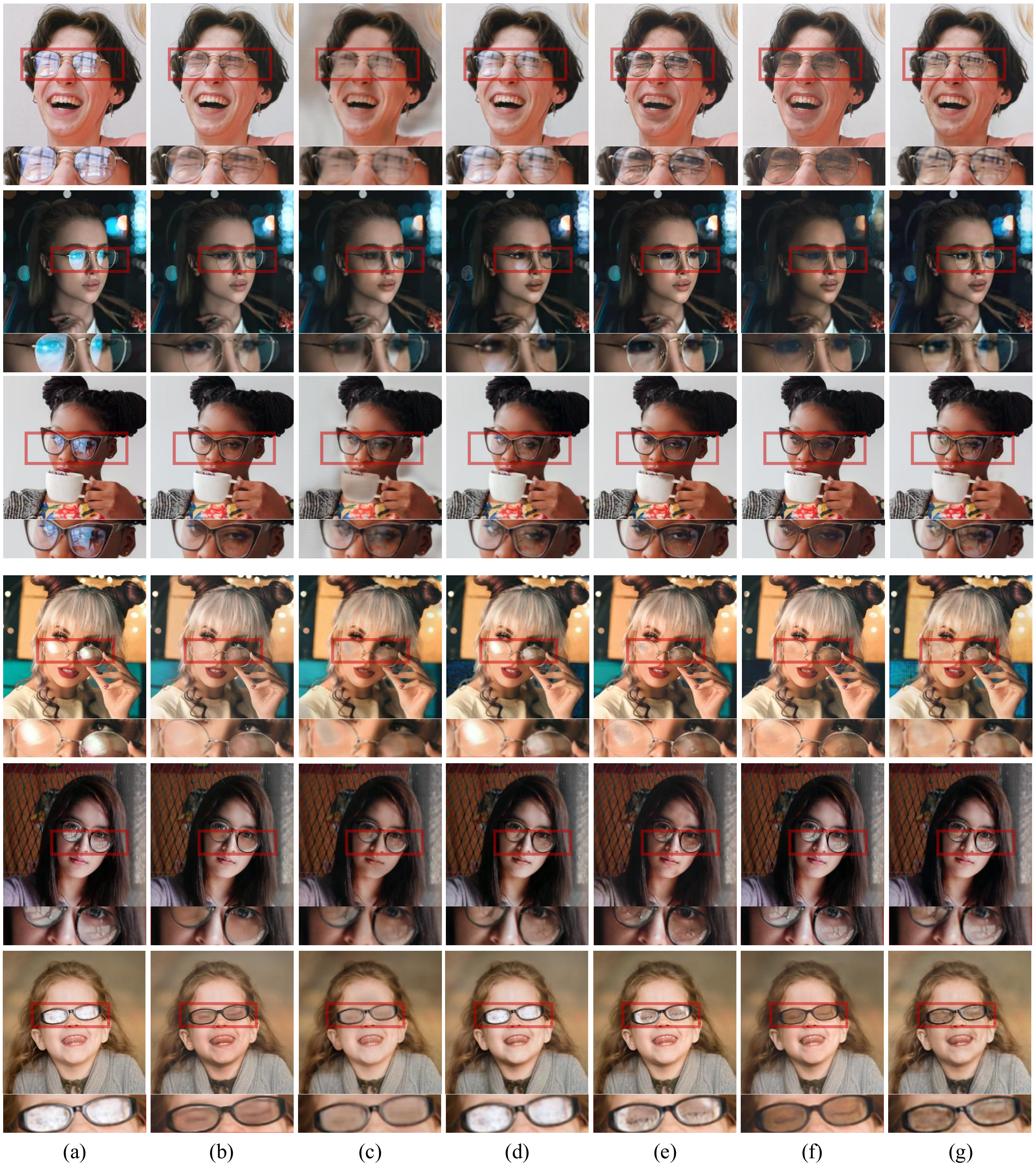

Figure 4. Qualitative comparison with other methods on images collected from the Internet. (a) Input image, (b) Ours, (c) Watanabe *et al.* [6], (d) IBCLN [4], (e) Robust SIRR [5], (f) DSRNet [3], (g) ER^{2}Net [8].

size of 768×512 at most. When the image size reaches 1536×1024, the graphics card memory is insufficient to support the operation. Other methods can only process images up to a resolution of 1536×1024 at most.

We present the visualization results of the high-resolution images in Fig. 6, from which we can observe the results of the comparison methods obtained are unsatisfied (from the results presented in Fig. 6). While our method employ the local structure sampling strategy to restore the details, and thus it can overcome the memory limitation to some extent and obtain more satisfied result.

4. More Visualization Results on Specular Highlights

Fig. 7 shows the comparison results of our method with other methods. It can be seen that our method can better eliminate specular highlights and restore texture details at the same time. Other methods do not completely eliminate specular highlights, and texture details are distorted.

References

[1] Gang Fu, Qing Zhang, Lei Zhu, Ping Li, and Chunxia Xiao. A multi-task network for joint specular highlight detection and removal. In *Proceedings of the IEEE/CVF Conference on Computer Vision and Pattern Recognition*, pages 7752–7761, 2021. 7

[2] Gang Fu, Qing Zhang, Lei Zhu, Chunxia Xiao, and Ping Li. Towards high-quality specular highlight removal by leveraging large-scale synthetic data. In *Proceedings of the IEEE/CVF International Conference on Computer Vision*, pages 12857–12865, 2023. 7

[3] Qiming Hu and Xiaojie Guo. Single image reflection separation via component synergy. In *Proceedings of the IEEE/CVF International Conference on Computer Vision*, pages 13138–13147, 2023. 1, 2, 3, 5

[4] Chao Li, Yixiao Yang, Kun He, Stephen Lin, and John E Hopcroft. Single image reflection removal through cascaded refinement. In *Proceedings of the IEEE/CVF Conference on Computer Vision and Pattern Recognition*, pages 3565–3574, 2020. 1, 2, 3, 5, 6

[5] Zhenbo Song, Zhenyuan Zhang, Kaihao Zhang, Wenhan Luo, Zhaoxin Fan, Wenqi Ren, and Jianfeng Lu. Robust single image reflection removal against adversarial attacks. In *Proceedings of the IEEE/CVF Conference on Computer Vision and Pattern Recognition*, pages 24688–24698, 2023. 1, 2, 3, 5, 6

[6] Sota Watanabe and Makoto Hasegawa. Reflection removal on eyeglasses using deep learning. In *2021 36th International Technical Conference on Circuits/Systems, Computers and Communications (ITC-CSCC)*, pages 1–4. IEEE, 2021. 1, 2, 3, 5, 6

[7] Zhongqi Wu, Chuanqing Zhuang, Jian Shi, Jianwei Guo, Jun Xiao, Xiaopeng Zhang, and Dong-Ming Yan. Single-image specular highlight removal via real-world dataset construction. *IEEE Transactions on Multimedia*, 24:3782–3793, 2021. 7

[8] Wentao Zou, Xiao Lu, Zhilv Yi, Ling Zhang, Gang Fu, Ping Li, and Chunxia Xiao. Eyeglass reflection removal with joint learning of reflection elimination and content inpainting. *IEEE Transactions on Circuits and Systems for Video Technology*, 34(10):10266–10280, 2024. 1, 2, 3, 5, 6

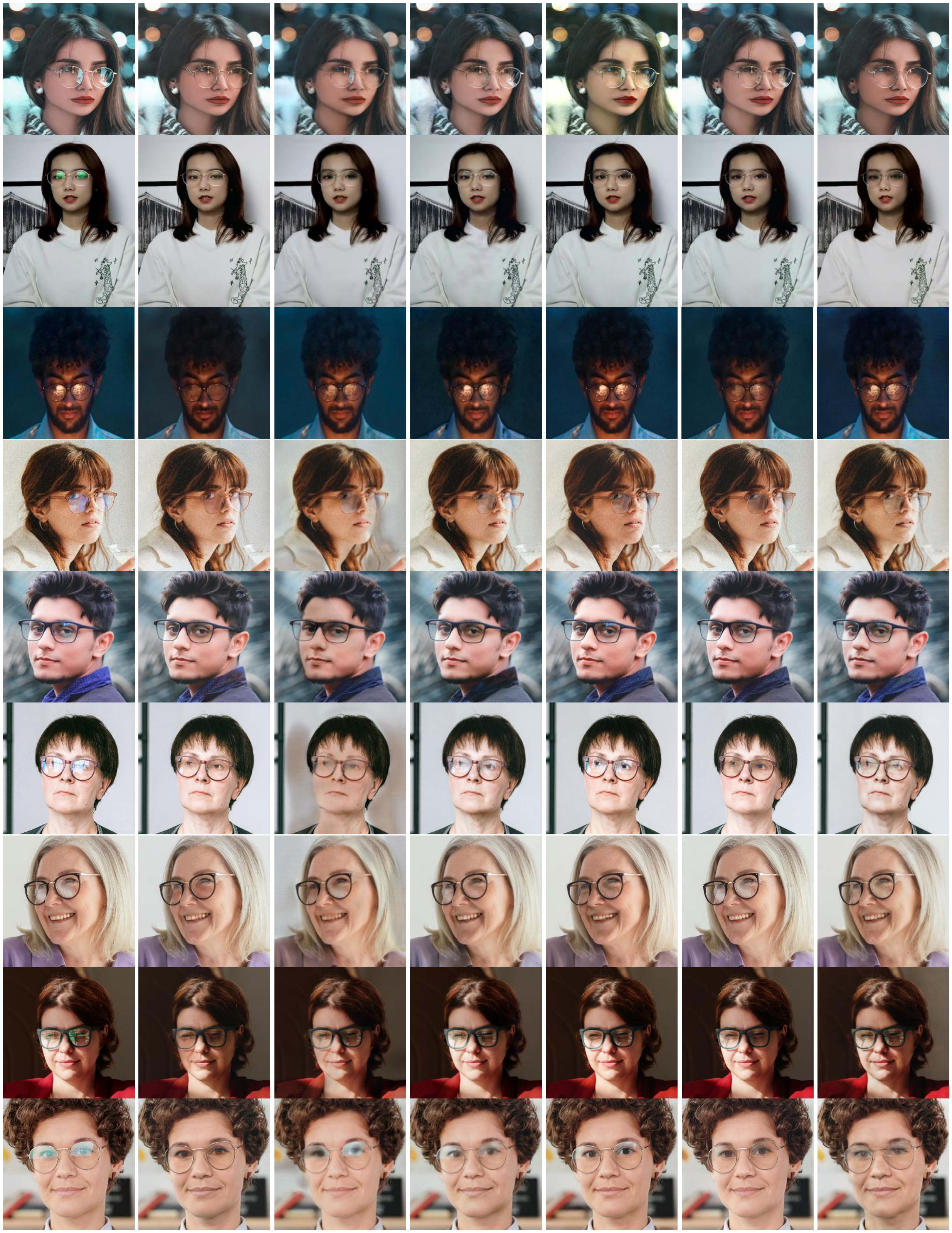

(a) (b) (c) (d) (e) (f) (g)

Figure 5. Qualitative comparison with other methods on images collected from the Internet. (a) Input image, (b) Ours, (c) Watanabe *et al.* [6], (d) IBCLN [4], (e) Robust SIRR [5], (f) DSRNet [3], (g) ER^{2}Net [8].

CVPR
#12127

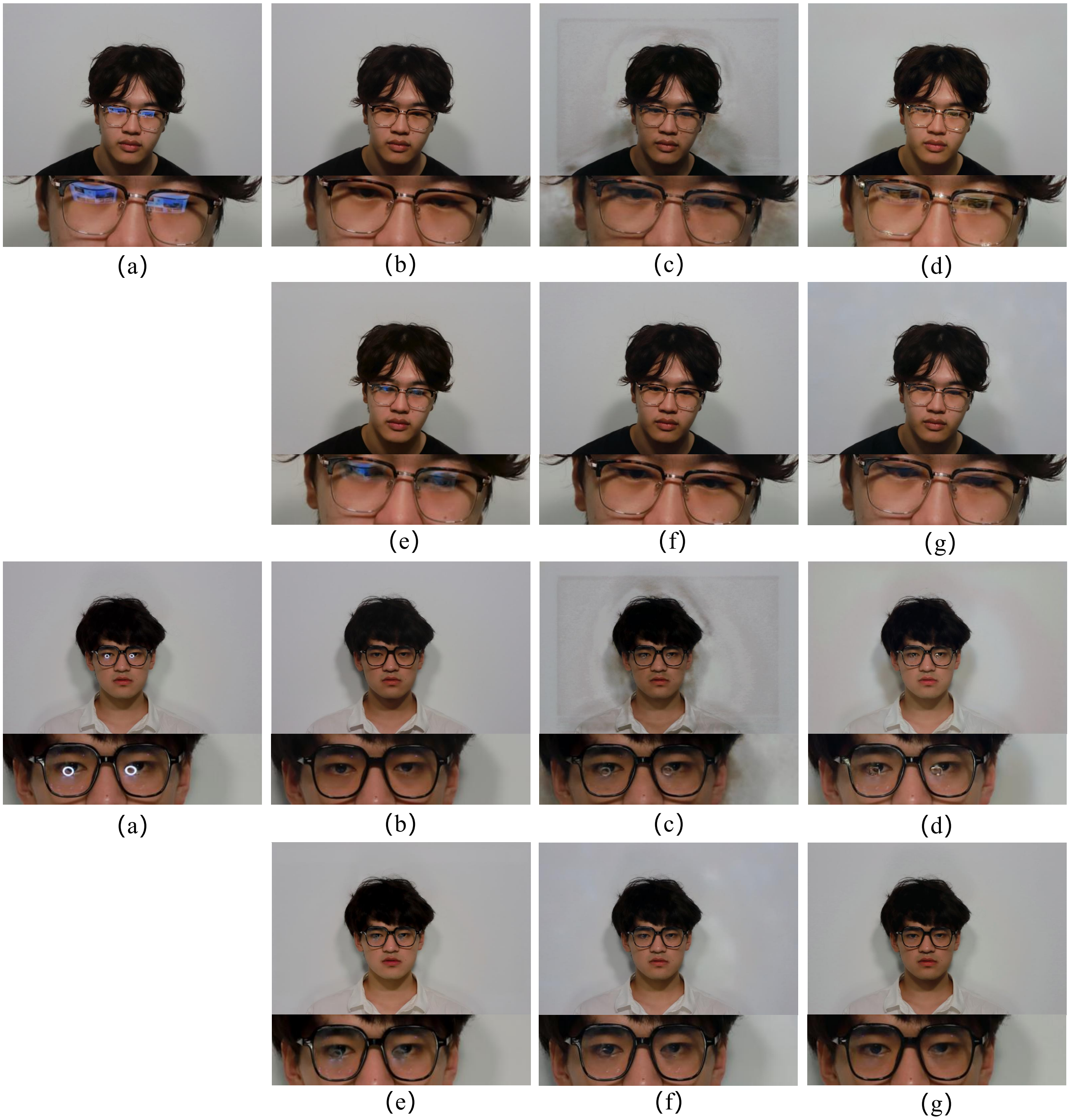

Figure 6. Visualization results on image with resolution of 1536×1024. (a) Input image, (b) GT, (c) IBCLN [4], (d) Robust SIRR [5], (e) ER^2Net [8], (f) Watanabe *et al.* [6], (g) Ours.

(a) (b) (c) (d) (e) (f)

Figure 7. Comparison with specular highlight removal methods. (a) Input, (b) GT, (c) Ours, (d) TSHRNet [2], (e) JSHDR [1], (f) SpecularityNet [7].